AD-A275 858

(1)

REPORT DOCUMENTATION PAGE

Form Approved
OMB No. 0704-0188

Public reporting burden for this collection of information is estimated to average 1 hour per response, including the time for reviewing instructions, searching existing data sources, gathering and maintaining the data needed, and completing and reviewing the collection of information. Send comments regarding this burden estimate or any other aspect of this collection of information, including suggestions for reducing this burden, to Washington Headquarters Services, Directorate for Information Operations and Reports, 1215 Jefferson Davis Highway, Suite 1204, Arlington, VA 22202-4302, and to the Office of Management and Budget, Paperwork Reduction Project (0704-0188), Washington, DC 20503

1. AGENCY USE ONLY (Leave blank)	2. REPORT DATE	3. REPORT TYPE AND DATES COVERED
	January 1994	Professional Paper

4. TITLE AND SUBTITLE

EXISTENCE AND UNIQUENESS OF MOTION PARAMETERS IN ACTIVE RANGING

5. FUNDING NUMBERS

PR: ZW02
PE: 0601152N
WU: DN308098

6. AUTHOR(S)

R. L. Ricks, S. Chatterjee

7. PERFORMING ORGANIZATION NAME(S) AND ADDRESS(ES)

Naval Command, Control and Ocean Surveillance Center (NCCOSC)
RDT&E Division
San Diego, CA 92152-5001

8. PERFORMING ORGANIZATION REPORT NUMBER

9. SPONSORING/MONITORING AGENCY NAME(S) AND ADDRESS(ES)

Office of Chief of Naval Research (OCNR)
Independent Research Programs
OCNR-10P
Arlington, VA 22217-5000

DTIC
ELECTE
FEB 18 1994
S C D

10. SPONSORING/MONITORING AGENCY REPORT NUMBER

11. SUPPLEMENTARY NOTES

12a. DISTRIBUTION/AVAILABILITY STATEMENT

Approved for public release; distribution is unlimited.

12b. DISTRIBUTION CODE

13. ABSTRACT (Maximum 200 words)

This paper discusses motion estimation of distributed objects. Measurements include position plus Doppler. We show that 2-D position plus Doppler is sufficient to uniquely determine the motion parameters of an object on a circular trajectory except for special cases. The uniqueness enhances occlusion tolerance and implies an approach to associating features. We show that the sensitivity of calculated motion parameters to measurement error is bounded. We also show that the error in the motion parameters tends to zero as the measurement error approaches zero.

DTIC QUALITY INSPECTED 3

94-05312

94 2 17 034

Published in *IEEE Transactions on Aerospace and Electronic Systems*, Vol. 30, No. 1, January 1994, pp. 18-29.

14. SUBJECT TERMS	15. NUMBER OF PAGES
motion analysis sonar	16. PRICE CODE

17. SECURITY CLASSIFICATION OF REPORT	18. SECURITY CLASSIFICATION OF THIS PAGE	19. SECURITY CLASSIFICATION OF ABSTRACT	20. LIMITATION OF ABSTRACT
UNCLASSIFIED	UNCLASSIFIED	UNCLASSIFIED	SAME AS REPORT

Best
Available
Copy

21a. NAME OF RESPONSIBLE INDIVIDUAL	21b TELEPHONE *(include Area Code)*	21c OFFICE SYMBOL
R. L. Ricks	(619) 553-1646	Code 572

Existence and Uniqueness of Motion Parameters in Active Ranging

ROCKIE L. RICKS
Naval Command, Control and Ocean Surveillance Center

SHANKAR CHATTERJEE
University of California, San Diego

Motion estimation of distributed objects is discussed. Measurements include position plus Doppler. We show that 2-D position plus Doppler is sufficient to uniquely determine the motion parameters of an object on a circular trajectory except for special cases. The uniqueness enhances occlusion tolerance and implies an approach to associating features. We show that the sensitivity of calculated motion parameters to measurement error is bounded. We also show that the error in the motion parameters tends to zero as the measurement error approaches zero.

Accesio
NTIS
DTIC
Unannc
Justific

By
Distribution /
Availability Codes
Dist | Avail and / or Special
A-1 | 20

Manuscript received April 10, 1990; revised October 1, 1992 and February 9, 1993.

IEEE Log No. T-AES/30/1/13042.

This work was supported by the Independent Research Program at Naval Command, Control and Ocean Surveillance Center, Research, Development, Test, and Evaluation Division and the Office of Naval Research.

Authors' current address: R. Ricks, [1]NCCOSC RDT& E Div., Code 572, 49590 Lassing Rd., San Diego, CA 92152-6147, [2]Computer Laboratory for Analyzing Spatial Signals, Department of Electrical and Computer Engineering, Mail Code R0407, University of California San Diego, La Jolla, CA 92037-0407; S. Chatterjee, Computer Laboratory for Analyzing Spatial Signals, Department of Electrical and Computer Engineering, Mail Code R0407, University of California San Diego, La Jolla, CA 92037-0407.

0018-9251/94/$4.00 © 1994 IEEE

I. INTRODUCTION

An object may be treated as a point scatterer for motion estimation of small (distant) objects. We define a distributed object as one that cannot be adequately represented as a single point scatterer for motion estimation purposes. A distributed object model is valid if the size of the object is of the same order as the distance between the object and the observer.

Many papers on motion estimation of distributed objects have appeared in the literature. See [19] for a more thorough review. The measurements are extracted from sequential images (or frames). Papers in the literature have dealt with a variety of measurement systems including perspective projections [4–8, 10–14], orthographic projections (3-D position) [2, 3, 15, 18], and range-Doppler [9]. Here we deal with a measurement vector that includes the 3-D (or 2-D) position plus Doppler. Such measurements are available from monopulse radar, and some sonar and laser systems.

A distributed object can be modeled as a surface or as a finite set of point scatterers [1]. The point scatterer model is more appropriate when the wavelength is shorter than object features. Here, we assume the point scatterers model. We also assume the scatterers are fixed on the object (i.e., rigid body motion).

There are two main approaches to motion estimation in the literature, flow-based methods and feature matching methods. For the point scatterer model of a distributed object, feature matching seems to be a natural choice.

Feature matching methods require that a correspondence be known or established between features in successive frames. Algorithms that do not require the establishment of correspondences have also been pursued [2, 3], but lack the occlusion tolerance and motion parameter uniqueness of the approach described here. Methods for establishing such correspondences have been developed in [8, 9, 13]. The process of establishing correspondences is prone to error. The probability of making an error is especially high when estimating motion from the first two frames if a prior motion estimate is not available. Errors from feature mismatch often propagate many frames before being resolved [9, 13].

On startup, rather than attempt to match features by the nearest neighbor method, we propose assuming feature associations over enough time samples such that the combined measurements uniquely determine the motion parameters. If motion parameters are calculated from the combined measurements, the motion parameters from each correctly associated feature are identical except for noise effects. If there are N features, there are N^2 possible feature associations between two frames of data. If three frames of data are required to uniquely determine the

motion parameters, one would have to consider N^3 associations. We choose to consider only two frames and only salient features such that N is small. To have sufficient measurements from only two frames we assume the measurements include position (i.e., active rather than passive measurements) plus Doppler. The use of only passive measurements would require more frames to uniquely determine the parameters of the same motion model. It would also require proof that the parameters of this specific motion model are uniquely determined. We show that only one feature match (6 measurements in 2-D) is required to uniquely estimate circular motion in a plane (5 unknown parameters). This analysis is extended to motion of a 3-D object when the orientation of the axis of rotation is known.

Occlusion (part of the object not visible) complicates the association of features. It may be caused by glint (phase interference) or one object shadowing another. It may occur if the transmitting and receiving beams are poorly positioned or insufficiently wide to cover the entire object. It may also be caused by aspect dependence or range dependence of the feature scattering strength as in the following examples. Consider a scenario where the range to the object is decreasing by orders of magnitude. The number of resolvable features increases as the range decreases. Consider also a scenario where the aspect is changing with time. Features visible at one aspect may not be visible at another.

Robustness against occlusion by filling in missing measurements with model estimates has been proposed [13]. This assumes a good motion estimate is available and the number of features is constant. To develop an algorithm that adapts to changes in the number and visibility of features, we propose matching features one by one and extracting the motion information from each match. Thus, the number of features and some (but not all) of the features being measured are allowed to change each frame.

Occlusion invalidates several common assumptions. It is common to represent the interframe motion as a rotation and a translation, and estimate the translation by assuming the average of the feature locations is fixed with respect to the object [2, 3, 9, 18]. Under occlusion the average of the feature locations is not fixed. It is frame dependent even without consideration of measurement noise. Object-centered coordinate systems [13–15] are inherently intolerant of occlusion.

Because the size of the object is of the order of the range, Doppler cannot be treated as "cross-range" as is commonly done in radar. For this work, Doppler is treated as a measurement of range-rate. Inclusion of Doppler as a measurement invariably leads to a nonlinear relationship between measurements and the estimated motion parameters. Therefore uniqueness is not guarenteed and it is necessary to analyze the existence and uniqueness of the motion parameters.

The work is organized as follows. In Section II the measurements are discussed. In Section III the motion model is given with insights into the limits that are placed on the model by the occlusion assumption. This is followed in Section IV by analysis of the uniqueness and existence of the motion parameter given the measurements. Finally, in Section V the sensitivities of the calculated motion parameters to errors in measurements are derived.

II. MEASUREMENTS

The measurement model is intended for an active (transmitting and receiving) system where the transmitted waveform is sufficiently narrow in bandwidth so that the time compression of the waveform due to motion of the object can be interpreted as a Doppler shift. Given that assumption, range-rate can be calculated exactly from the transmitted and received frequencies, f_t and f_r by

$$\dot{r} = c\frac{f_r - f_t}{f_r + f_t} \tag{1}$$

where c is the speed of the sound.

We assume the system has two sensors on the order of a wavelength apart. The direction of arrival can be estimated from the difference in phase between sensors. The wavelength is assumed small with respect to the object structure so the sonar return is dominated by specular reflections, thus justifying the representation of the object as a set of point scatterers. We also assume that the resolution of the transmitted pulse is sufficient to resolve the features of the object.

III. MOTION MODELS

Models for motion estimation of point objects use parameters such as position and velocity. A motion model for distributed objects must describe the motion of each feature on the object. One could build a distributed model by letting each point have its own motion parameters and add the constraint that feature-to-feature fluctuations in the parameters are small. Rather than add this complexity, we assume the motion parameters are constants.

One approach to representing distributed motion with constant parameters is to describe the motion of a reference point on the object and the relation of all features to it. Another approach is to describe the motion of the whole rigid object such that the motion parameters describe the motion of each and every feature on the object. An equivalent definition is that the parameters that describe the motion of the object as a whole are observable from measurements of any feature on the object. The motion parameters in

such a model are herein called "common" motion parameters.

The reference point model is poorly defined when the reference point is not directly measurable. If an arbitrary point on the object is chosen, the position of that point can be updated with time using estimated motion parameters. With uncertainty in the motion parameters, the measurement uncertainty of the reference position always increases with time. Unless measurements of the reference point's position can be obtained, the reference point model is not viable for estimation purposes. If the reference point is an object feature, that feature may become unmeasurable due to occlusion. If the reference point is the object centroid (average of all visible features), its measurement is affected by the occlusion of any feature. In our model, we assume that the features are fixed on the object and are visible for at least two successive frames. The centroid is allowed to vary from frame to frame. To add robustness against occlusion, the common motion model is used for motion estimation.

However, the common motion model also has a drawback. The common motion model for a circular (rotating) trajectory is poorly defined for a straight-line (nonrotating) trajectory. The reference point model is well defined on the boundary between circular and straight-line trajectories. It is used to generate common motion models for both circular and straight-line trajectories. Therefore both common motion models represent equivalent motion at the boundary.

To derive the reference point motion model we assume the object is moving with a constant angular-velocity on a circular trajectory in a known plane [20]. Five parameters are needed to describe the motion of the reference point; the initial position x_0, y_0, speed V, initial heading h_0, and heading rate ω.

For a distributed object, we add structure, the position of the additional features relative to the reference point which is denoted as (u_i, v_i) where u_i is the position component of the ith feature in the direction of the heading and v_i is the component along the perpendicular direction as shown in Fig. 1. The position, $P_i(t)$, and range-rate, $\dot{r}_i(t)$, for the ith feature without noise are given by

$$x_i(t) = x_0 + u_i \cos h(t) - v_i \sin h(t) + V \int_0^t \cos h(\tau)\, d\tau \tag{2}$$

$$y_i(t) = y_0 + u_i \sin h(t) + v_i \cos h(t) + V \int_0^t \sin h(\tau)\, d\tau \tag{3}$$

$$h(t) = h_0 + \omega t \tag{4}$$

$$P_i(t) = [x_i(t) \quad y_i(t)]^{\mathrm{T}} \tag{5}$$

$$\dot{r}_i(t) = P_i(t)^{\mathrm{T}} \dot{P}_i(t) / \|P_i(t)\| \tag{6}$$

where T denotes the transpose.

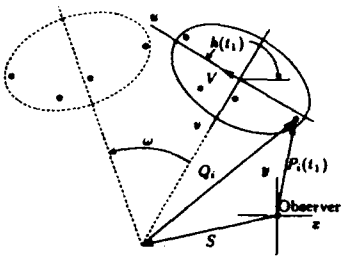

Fig. 1. "Common" parameter motion model of distributed object.

Note that the observer need not be at the center of the circle. The heading rate ω, and the center of rotation S are common motion parameters. They are the same for all features on the object. With the designation of an increment in time, they constitute a transformation. Furthermore, the parameters (of the transformation) are time invariant. The relation between the reference point model and the common motion model is as follows:

$$S = \begin{bmatrix} x_0 - \dfrac{V}{\omega} \sin h_0 \\ y_0 + \dfrac{V}{\omega} \cos h_0 \end{bmatrix} \tag{7}$$

$$Q_i = \begin{bmatrix} u(i) \\ v(i) - \dfrac{V}{\omega} \end{bmatrix} \tag{8}$$

$$H_0 = \begin{bmatrix} \cos h_0 & -\sin h_0 \\ \sin h_0 & \cos h_0 \end{bmatrix} \tag{9}$$

$$R_\omega(t) = \begin{bmatrix} \cos \omega t & -\sin \omega t \\ \sin \omega t & \cos \omega t \end{bmatrix} \tag{10}$$

$$P_i(t) = S + R_\omega(t) H_0 Q_i. \tag{11}$$

The model can be further simplified by letting $G_i = H_0 Q_i$ which yields

$$P_i(t) = S + R_\omega(t) G_i. \tag{12}$$

This simplification leads to no loss of generality because the matrix H_0 only orients the object-centered coordinate system.

As mentioned, this parameterization has a drawback. As the heading rate approaches zero, the distance between the object and the center of rotation approaches infinity. For this case (straight-line motion) a different common motion model is used. The reference point model with $\omega = 0$ is equivalent to the following common motion model with the velocity components, $V_x = V \cos(h_0)$ and $V_y = V \sin(h_0)$, as the common motion parameters. The model becomes

$$P_i(t) = \begin{bmatrix} x_0 \\ y_0 \end{bmatrix} + H_0 \begin{bmatrix} u_i \\ v_i \end{bmatrix} + \begin{bmatrix} V_x \\ V_y \end{bmatrix} t. \tag{13}$$

The range-rate measurement is given by (6). For straight-line motion, there is no need to distinguish

between the common motion and the reference point models.

IV. EXISTENCE AND UNIQUENESS

The relationship between parameters and measurements for the circular trajectory, common motion model is nonlinear. Therefore, having more measurements than unknowns is not sufficient to establish the uniqueness of the motion parameter solution. Furthermore, a solution may not exist. In this section both existence and uniqueness of the common motion parameters are analyzed for an object on a circular trajectory. A method is given to distinguish straight-line and circular trajectories. Once a straight-line trajectory is distinguished, the existence and uniqueness analysis becomes trivial with position measurements only. We concentrate on analyzing the circular trajectory while extending some analysis to straight-line trajectories.

Circular motion cannot be uniquely determined from position measurements at two successive times. (An infinite number of circles can be drawn through two points.) The ambiguity is resolved using range-rate measurements in addition to position.

Let the ith object feature be observed through 2-D position $P_i(t)$ and range-rate $\dot{r}_i(t)$ (from Doppler) measurements at successive times $t = t_1, t_2$ given by

$$P_i(t) = S + R_\omega(t)G_i \tag{14}$$

$$\dot{r}_i(t) = P_i(t)^T \dot{P}_i(t)/\|P_i(t)\|. \tag{15}$$

Beginning with these six measurement equations in the five unknown motion parameters, ω, S, and G_i, we use substitution to reduce the problem to two transcendental equations in the one unknown parameter ω. Differentiation of $P_i(t)$ gives

$$\dot{P}_i(t) = \dot{R}_\omega(t)G_i \tag{16}$$

$$= \omega B R_\omega(t)G_i \tag{17}$$

where

$$B = \begin{bmatrix} 0 & -1 \\ 1 & 0 \end{bmatrix}. \tag{18}$$

The change in position is

$$\Delta P_i = P_i(t_2) - P_i(t_1) \tag{19}$$

$$= (R_\omega(t_2) - R_\omega(t_1))G_i \tag{20}$$

$$= 2\sin(\omega t_d) B R_\omega(t_a) G_i \tag{21}$$

where $t_a = (t_2 + t_1)/2$ and $t_d = (t_2 - t_1)/2$. Substituting (21) into (17) to eliminate G_i and substituting for $\dot{P}_i(t)$ gives the pair of equations

$$\dot{r}_i(t_k) = (\omega P_i(t_k)^T R_\omega(t_k - t_a)\Delta P_i)/(2\|P_i(t_k)\|\sin\omega t_d), \quad k = 1,2 \tag{22}$$

where the subscript k has been added to distinguish equations. Both equations are clearly a function of both t_1 and t_2. Further simplification is possible using $p = \omega t_d$ to scale ω and defining

$$A_i(t_k) = \|\Delta P_i\|/(2t_d|\dot{r}_i(t_k)|) \tag{23}$$

$$\psi_i(t_k) = \operatorname{sgn}(t_k - t_a)\theta_i(t_k) + \frac{\pi}{2} - \frac{\pi}{2}\operatorname{sgn}(\dot{r}_i(t_k)) \tag{24}$$

$$\theta_i(t_k) = \arctan\left[\frac{P_i(t_k)^T B \Delta P_i}{P_i(t_k)^T \Delta P_i}\right] \tag{25}$$

$$\operatorname{sgn}(t) = \begin{cases} 1 & t > 0 \\ -1 & t \le 0 \end{cases}. \tag{26}$$

These substitutions yield

$$\sin p/p = A_i(t_k)\cos(p - \psi_i(t_k)), \quad k = 1,2 \tag{27}$$

which is the basis of our uniqueness and existence analysis. Since (27) is really two equations, for clarity we use the word roots to mean the solution of a single equation. We use the word solution in referring to both equations simultaneously. Because the above derivation involved dividing by $\dot{r}_i(t_k)$, special considerations are required when $\dot{r}_i(t_k) = 0$.

If we let $\hat{p}$ be the solution of (27), the center of rotation is

$$\hat{S} = [P_i(t_1) + P_i(t_2)]/2 + (\cot(\hat{p})/2)B\Delta P_i. \tag{28}$$

Clearly $\hat{S}$ exists and is unique if a solution of (27), $\hat{p}$, exists and is unique, respectively. Therefore the focus is on the existence of a solution to (27) and its uniqueness.

A. Motion Classes

We define the following exceptional classes of motion. Let $\mathcal{C}_1$ be straight-line motion. Let $\mathcal{C}_2$ be circular motion for a feature that is the center of rotation ($\|G_i\| = 0$). Let $\mathcal{C}_3$ be circular motion for a feature that has completed a full circle between samples ($p = n\pi$, $n \neq 0$, $n \in \mathcal{N}$). Let $\mathcal{C}_4$ be the nil motion of a stationary feature. $\mathcal{C}_4$ can be mathematically described by the straight-line motion parameters with $V_x = V_y = 0$. Note that (21) and (17) are not valid for motion classes $\mathcal{C}_1$ and $\mathcal{C}_4$. There is reason for concern that (27) does not apply to this case. However, by substituting the common motion model for straight-line motion into (27) we get

$$\sin p/p = \cos p + \sin p \operatorname{sgn}(t_k - t_a)\tan(\theta_i(t_k)) \quad k = 1,2. \tag{29}$$

Clearly $p = 0$ is always a root. Therefore (27) is valid for $\mathcal{D}_i \in \mathcal{C}_1$.

Define $\mathcal{D}_i$ as the motion class of the ith feature. The following lemmas determine if $\mathcal{D}_i$ belongs to exceptional classes $\mathcal{C}_2$, $\mathcal{C}_3$, or $\mathcal{C}_4$.

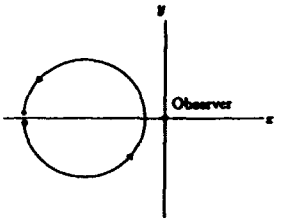

Fig. 2. Object feature on a circular trajectory and observer outside the circle.

LEMMA 1 *Motion classes C_2 and C_4 are physically indistinguishable.*

LEMMA 2 $\mathcal{D}_i \in C_3 \Rightarrow \|\Delta P_i\| = 0$.

LEMMA 3 $\mathcal{D}_i \in C_2 \cup C_4 \Rightarrow \|\Delta P_i\| = 0$ *and* $\dot{r}_i(t) = 0$.

LEMMA 4 $\|\Delta P_i\| = 0 \Rightarrow \mathcal{D}_i \in C_2 \cup C_3 \cup C_4$.

PROOF. Using the circular motion model, the proof for motion classes C_2 or C_3 follows from

$$\Delta P_i^T \Delta P_i = 4\sin^2 p \; G_i^T G_i. \tag{30}$$

Using the straight-line motion model, the proof for motion class C_4 follows from

$$\Delta P_i^T \Delta P_i = 4t_d^2(V_x^2 + V_y^2). \tag{31}$$

□

By Lemma 4, if $\|\Delta P_i\| = 0$ we conclude $\mathcal{D}_i \in C_2 \cup C_3 \cup C_4$. But if $\|\Delta P_i\| = 0$ and $\dot{r}_i(t_k) \neq 0$, $k = 1$ or 2 we further conclude $\mathcal{D}_i \in C_3$. However, there exists a subset of C_3 such that $\dot{r}_i(t_k) = 0$, $k = 1,2$ which is visibly indistinguishable from $C_2 \cup C_4$.

B. Existence of Motion Parameter Solution

Assume $\mathcal{D}_i \notin C_2 \cup C_3 \cup C_4$. The measurements enter into (27) only through the functions $A_i(t_k)$ and $\psi_i(t_k)$. Given $P_i(t_k)$, $\Delta P_i \in \mathcal{R}^2 - \{(0,0)\}$ and $\dot{r}_i(t_k) \in [-M, M]$ for an appropriate value M, $A_i(t_k)$ and $\psi_i(t_k)$ map onto the intervals $(0,\infty)$ and $(p-\pi, p+\pi]$, respectively. Their domains are more restricted in special cases.

Consider a feature moving on a circular trajectory with the observer outside the circle as shown in Fig. 2. In Figs. 2–7 the trajectory of $P_i(t_1)$ begins at the "o" and ends at the "*." The trajectory of $P_i(t_2)$ leads that of $P_i(t_1)$ by the angle $2p$. Here $p = 0.4$. As the feature moves, $\psi_i(t_1)$ and $\psi_i(t_2)$ take on sampled values along the trajectory shown in Fig. 3. As a feature completes one circle, $\psi_i(t_1)$ cycles through its domain twice.

If the observer is inside the trajectory circle as shown in Fig. 4, the trajectory of $\psi_i(t_1)$ changes form as shown in Fig. 5. Variables $\psi_i(t_k)$, $k = 1,2$ never take on values on the interval $(p - \arccos(d_0/d), p + \arccos(d_0/d))$.

For a feature on a straight-line trajectory, the trajectory and corresponding $\psi_i(t_1)$ and $\psi_i(t_2)$ trajectories are shown in Figs. 6 and 7. Here $\psi_i(t_1)$ and $\psi_i(t_2)$ take on the value zero only if the observer is in the path of the feature trajectory. They approach zero as the feature range ($\|P_i(t_1)\|$ or $\|P_i(t_2)\|$) approaches infinity.

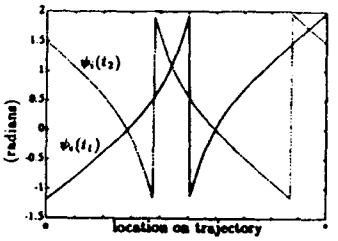

Fig. 3. Trajectories of $\psi_i(t_1)$ and $\psi_i(t_2)$ for circular feature trajectory and observer outside the circle.

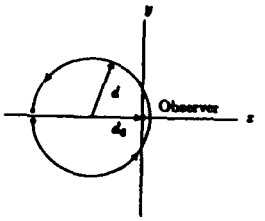

Fig. 4. Object feature on a circular trajectory and observer inside the circle.

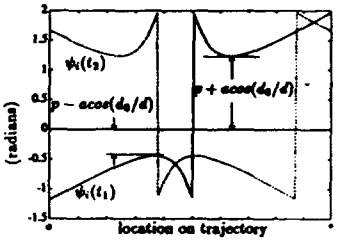

Fig. 5. Trajectories of $\psi_i(t_1)$ and $\psi_i(t_2)$ for circular feature trajectory and observer inside the circle.

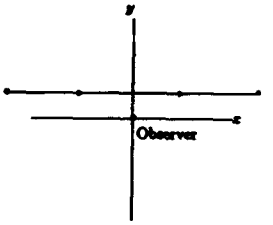

Fig. 6. Object feature on a straight-line trajectory.

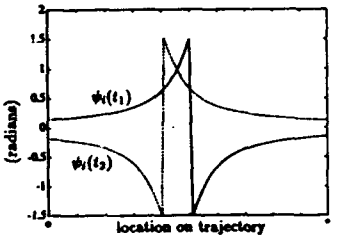

Fig. 7. Trajectories of $\psi_i(t_1)$ and $\psi_i(t_2)$ for straight-line feature trajectory.

TABLE 1
Values of $A_{crit}(\psi_i(t_k))$

m	A_{crit} $(m\pi/30)$	m	A_{crit} $(m\pi/30)$
0	1.00000	8	0.82808
1	0.99726	9	0.79330
2	0.98905	10	0.73442
3	0.97541	11	0.67822
4	0.95638	12	0.61707
5	0.93206	13	0.54839
6	0.90251	14	0.46743
7	0.86783	15	0.31831

With these preliminaries, we next investigate the existence of roots of (27) for each k separately. Conditions for existence of roots are as follows.

THEOREM 1 *If $|(\psi_i(t_k))_{2\pi}| < \pi/2$ there is a value $A_{crit} = A_{crit}(\psi_i(t_k))$ that satisfies the following: Equation (27, $t = t_k$) has two roots on the interval $p \in (-\pi\ \pi]$ iff $A_i(t_k) \geq A_{crit}$.*

The subscript 2π indicates constraint modulo 2π to the interval $(-\pi,\pi]$. The proof is shown graphically in Fig. 8. Note the main lobe of the $\sin p/p$ always has twice the width of the sinusoid.

COROLLARY 1 *If $|(\psi_i(t_k))_{2\pi}| < \pi/2$ and two roots of (27, $t = t_k$) exist on the interval $p \in (-\pi,\pi]$, those roots are identical iff $A_i(t_k) = A_{crit}$.*

$A_i(t_k) = A_{crit}(\psi_i(t_k))$ defines the boundary for the existence of roots to (27). If $A_i(t_k) < A_{crit}(\psi_i(t_k))$ no roots exist. However, for the noiseless case, $A_i(t_k)$ is always greater than or equal to $A_{crit}(\psi_i(t_k))$ and equality is only achieved if sample times happen to fall at specific time instants. The noisy measurement case is treated in Section V.

The function $A_{crit}(\psi_i(t_k))$ can be calculated numerically by noting that both functions in Fig. 8 and their derivatives are equal when $A_i(t_k) = A_{crit}(\psi_i(t_k))$. Let p_{crit} denote the value of p at the point of tangency. Then we can calculate $A_{crit}(\psi_i(t_k))$ from

$$A_{crit}^2(\psi_i(t_k)) = \frac{p_{crit}^2 + \sin^2 p_{crit} - 2p_{crit}\sin p_{crit}\cos p_{crit}}{p_{crit}^4} \tag{32}$$

$$\tan(\psi_i(t_k)) = \frac{p_{crit} - \sin p_{crit}\cos p_{crit}}{\sin^2 p_{crit}} \tag{33}$$

by solving (33) numerically for p_{crit}. Results are listed in Table I which is interpreted using $A_{crit}(x) = A_{crit}(-x)\ \forall x$. It is interesting to note that $A_{crit}(\pi/2) = 1/\pi$.

Theorem 1 with substitution from (23) gives an upper bound on the range rate of the ith feature,

$$|\dot{r}_i(t_k)| \leq \frac{\|\Delta P_i\|}{2t_d A_{crit}(\psi_i(t_k))} \tag{34}$$

as a sufficient and necessary condition for roots of (27) to exist if $|(\psi_i(t_k))_{2\pi}| < \pi/2$.

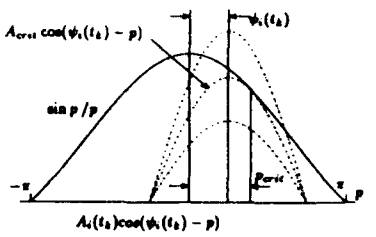

Fig. 8. Graph of (27) showing the existence of 0 or 2 roots as a function of $A_i(t_k)$.

Theorem 1 is useful for testing whether roots exist, but the following extension is more useful in proving the theorems that follow.

Let

$$\psi_i(t_k) = \xi(p_{crit}) = \arctan\left(\frac{p_{crit} - \sin p_{crit}\cos p_{crit}}{\sin^2 p_{crit}}\right) \tag{35}$$

represent the invertible mapping of (33).

THEOREM 2 *Given $\psi_i(t_k)$, $A_i(t_k) = A_{crit}$ iff $p = p_{crit} = \xi^{-1}(\psi_i(t_k))$.*

The proof follows from (32). Even though p_{crit} is a double-valued function of A_{crit}, the ambiguity is resolved by knowing the sign of $\psi_i(t_k)$.

Next we consider conditions for which roots always exist.

THEOREM 3 *If $-\pi < (\psi_i(t_k))_{2\pi} \leq -\pi/2$ or $\pi/2 \leq (\psi_i(t_k))_{2\pi} \leq \pi$, (27) has two roots on the interval $p \in (\pi,\pi]$.*

The proof also follows from Fig. 8.

If it is known a priori that the observer is inside the feature's circular trajectory, the following theorem is useful. With a sufficiently high sample rate (sufficiently small p), two roots always exist. Let $\zeta(p) = p - \xi(p)$. This is also an invertible mapping.

THEOREM 4 *If the observer is inside the circular trajectory of the feature and $|p| < \zeta^{-1}(\arccos(d_0/d))$ then $p \neq \xi^{-1}(\psi_i(t_k))\ \forall t_k$.*

PROOF OF THEOREM 4 The proof follows from Fig. 5. The function $\xi(p)$ is a monotonically increasing and passes through the origin. Therefore a plot of p_{crit} versus time has the same form as the plot of $\psi_i(t_k)$ in Fig. 5. It follow that there exists a value p_{m1} corresponding to $p - \arccos(d_0/d)$ in Fig. 5 such that p_{crit} never exceeds p_{m1} during the first half of the $\psi_i(t_1)$ trajectory. Similarly, there exists a value p_{m2} corresponding to $p + \arccos(d_0/d)$ in Fig. 5 such that p_{crit} never decreases below p_{m2} during the second half of the $\psi_i(t_1)$ trajectory. If p is such that $p_{m1} < p < p_{m2}$, then $p \neq p_{crit}\ \forall t_k$, $k = 1,2$. Transforming by applying $\xi(\cdot)$ yields

$$p - \arccos(d_0/d) < \xi(p) < p + \arccos(d_0/d) \tag{36}$$

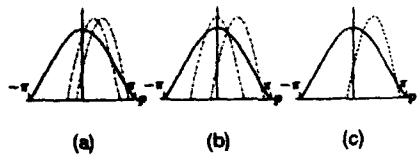

Fig. 9. Equation (27, $t = t_1$) is (a) inconsistent, (b) consistent with one root, and (c) consistent with both roots of (27, $t = t_2$).

and

$$|p| < \zeta^{-1}(\arccos(d_0/d)). \tag{37}$$

□

Consider the special case of $\dot{r}_i(t_k) = 0$. Equation (27) has the two roots $p = \psi_i(t_k) \pm \pi/2$. Clearly, roots always exist.

Consider the case of straight-line motion ($\mathcal{D}_i \in \mathcal{C}_1$). With the following minor conditions, two roots always exist.

THEOREM 5 *If the feature is on a straight-line trajectory, the observer is not located on the trajectory, and* $\|P_i(t_k)\| < \infty$, *then* $p \neq \xi^{-1}(\psi_i(t_k))$.

The proof follows from Fig. 7.

To this point, we have examined (27) for each time separately. Using (27) for both instants of time t_1 and t_2, we examine the existence as well as the uniqueness of the solution. The existence condition is stated as follows.

LEMMA 5 *If roots exist for both equations* (27, $k = 1$) *and* (27, $k = 2$), *a solution exists for* (27) *the pair iff one root of* (27, $k = 1$) *is identical to one root of* (27, $k = 2$).

This is illustrated in Fig. 9. In Fig. 8, (27) is plotted showing variations of $A_i(t_k)$. Here (27) is again plotted, but $A_i(t_k)$ is constant and both equations ($k = 1,2$) are shown.

Generally, it is a good idea to stay away from the existence boundary ($A_i(t) = A_{\text{crit}}$). We show that motion parameters are more sensitive to measurement error there. The following theorem gives conditions such that roots of both equations are simultaneously on the existence boundary.

THEOREM 6 *Assume the roots of* (27, $k = 1$) *are on the existence boundary and that the roots of* (27, $k = 2$) *satisfy the existence conditions of Lemma 5. Then the roots of* (27, $k = 2$) *are also on the existence boundary iff the object-observer geometry is one of the ambiguous geometries defined* $\psi_i(t_2) = \psi_i(t_1)$ *(discussed later).*

PROOF OF THEOREM 6 Although p is unknown, we know $p = p_{\text{crit}} = \xi^{-1}(\psi_i(t_k))$, $k = 1,2$. Applying the one to one mapping, ξ, yields

$$\psi_i(t_2) = \psi_i(t_1). \tag{38}$$

The converse is straight forward. □

C. Uniqueness of Motion Parameters

What if two values $p^{(1)}$ and $p^{(2)}$ exist which are roots of both equations (27, $k = 1$) and (27, $k = 2$)? The uniqueness of the solution is stated in the following theorem which is proved with the aid of subsequent lemmas.

THEOREM 7 *Let* $\theta_i(t_1)$ *be the angle between* $P_i(t_1)$ *and* ΔP_i, *and* $\theta_i(t_2)$ *be the angle between* $P_i(t_2)$ *and* ΔP_i ($\theta_i(t_1)$ *and* $\theta_i(t_2)$ *are consistent with earlier definitions.*) *Assume a solution exists for* (27). *The solution is ambiguous (two distinct solutions exist) iff*

$$\theta_i(t_1) + \theta_i(t_2) = 0, \qquad \dot{r}_i(t_2) = \dot{r}_i(t_1) \tag{39}$$

or

$$\theta_i(t_1) + \theta_i(t_2) = \pi, \qquad \dot{r}_i(t_2) = -\dot{r}_i(t_1). \tag{40}$$

LEMMA 6 *The equation*

$$A_i(t_1)\cos(p - \psi_i(t_1)) = A_i(t_2)\cos(p - \psi_i(t_2)) \tag{41}$$

is either true for all p, or has two solutions on the interval $p \in (-\pi, \pi]$ *and* $p^{(2)} = p^{(1)} + \pi$.[1]

To prove Lemma 6, we form a function by subtracting the right-hand side of (41) from the left-hand side. The function is a sinusoid of the same period and the roots are related by $p^{(2)} = p^{(1)} + \pi$. By application of the Intermediate Value Theorem to this function, we conclude it has two roots on $(-\pi, \pi]$, unless it is zero everywhere, in which case all values of p are roots.

LEMMA 7 *Two values,* $p^{(1)}$ *and* $p^{(2)} \neq p^{(1)}$, *exist which are roots of both* (27, $k = 1$) *and* (27, $k = 2$) *iff*

$$A_i(t_1)\cos(p - \psi_i(t_1)) = A_i(t_2)\cos(p - \psi_i(t_2)) \qquad \forall\ p. \tag{42}$$

PROOF OF LEMMA 7 If $p^{(1)}$ and $p^{(2)}$ are roots of both equations (27, $k = 1$) and (27, $k = 2$) and $p^{(1)} \neq p^{(2)}$, then

$$\frac{\sin p}{p} = A_i(t_1)\cos(p - \psi_i(t_1)) = A_i(t_2)\cos(p - \psi_i(t_2)), \qquad p = p^{(1)}, p^{(2)}. \tag{43}$$

Since $\sin p/p \geq 0$ for $p \in (-\pi, \pi]$ and $\sin p/p = 0$ only for $p = \pi$, we can assign the roots to $p^{(1)}$ and $p^{(2)}$ such that $A_i(t_k)\cos(p^{(1)} - \psi_i(t_k)) > 0$, $k = 1,2$ and $A_i(t_k)\cos(p^{(2)} - \psi_i(t_k)) \geq 0$, $k = 1,2$. Assume there exists some value $p \in (-\pi, \pi]$ such that (43) is not true. Then, given that $p^{(1)}$ satisfies (43), by Lemma 6,

[1] When angles are added, we imply that the result is constrained to the interval $(-\pi, \pi]$.

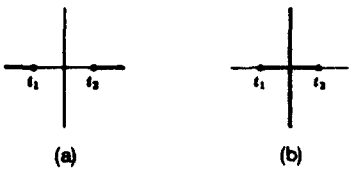

Fig. 10. Ambiguous geometries for (a) $\theta_i(t_1) + \theta_i(t_2) = 0$, and (b) $\theta_i(t_1) + \theta_i(t_2) = \pi$.

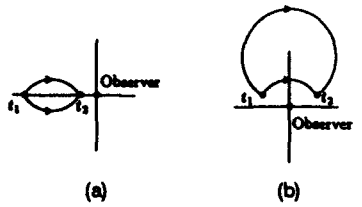

Fig. 11. Trajectories associated with ambiguous geometries. (a) Symmetric. (b) Asymmetric.

$p^{(2)} = p^{(1)} + \pi$ is the other root. This leads to the contradiction

$$A_i(t_k)\cos(p^{(1)} - \psi_i(t_k)) \leq 0 \qquad k = 1,2. \tag{44}$$

The converse follows from Fig. 9(c). □

LEMMA 8 *Since* $A_i(t_1), A_i(t_2) > 0$,

$$A_i(t_1)\cos(p - \psi_i(t_1)) = A_i(t_2)\cos(p - \psi_i(t_2)) \qquad \forall\ p$$

$$\Rightarrow \psi_i(t_1) = \psi_i(t_2). \tag{45}$$

PROOF OF THEOREM 7 Assume the solution is ambiguous (i.e., $p^{(1)}$ and $p^{(2)} \neq p^{(1)}$ are roots of both equations (27, $k = 1$) and (27, $k = 2$)). Then by Lemmas 7 and 8 $\psi_i(t_1) = \psi_i(t_2)$. First, if we assume $\dot{r}_i(t_2) = \dot{r}_i(t_1)$ in (24)

$$\theta_i(t_2) = -\theta_i(t_1). \tag{46}$$

Alternately, if we assume that $\dot{r}_i(t_2) = -\dot{r}_i(t_1)$ in (24)

$$\theta_i(t_2) = -\theta_i(t_1) + \pi. \tag{47}$$

To prove the converse, one can show that $\psi_i(t_1) = \psi_i(t_2)$ and $A_i(t_1) = A_i(t_2)$. We then conclude that

$$A_i(t_1)\cos(p - \psi_i(t_1)) = A_i(t_2)\cos(p - \psi_i(t_2)) \qquad \forall\ p \tag{48}$$

and the trajectory is ambiguous by Lemma 7. □

Assume an object feature is located as indicated by the "o"s in Fig. 10(a) and (b) at times $t = t_1$ and $t = t_2$. The loci of the observer locations that yield ambiguous geometries are shown as dark lines.

If measured positions and observer are collinear, the ambiguous trajectories are reflections of each other as shown in Fig. 11(a). If the observer lies on a perpendicular bisector of ΔP_i, the ambiguous trajectories are dissimilar as shown in Fig. 11(b). Ambiguities associated with nonsymmetric trajectories are resolved by measurements at another time t_3, if the trajectory is again limited to less than a full circle between t_2 and t_3. The speed distinguishes the correct trajectory.

It is possible that the ambiguity of a collinear geometry would not be resolved by a measurement at t_3 if the feature position is also collinear with the first two (and the observer). Since these are limited to specific ambiguous geometries, it is highly probable that ambiguities would be resolved by matching multiple features on an object.

D. Existence and Uniqueness for 3-D Position Plus Doppler

This analysis can be extended to 3-D motion if the orientation of the rotation axis is known. If the plane of object motion is unknown, a noncollinear position measurement at another time t_3 is required. Assume now that Doppler and 3-D position measurements are available. We consider the case where the observer is not in the plane of motion of a given feature. Assume that the observer is at $z = 0$ and the reference has been rotated such that measurements yield the same depth (i.e., $z_i(t_1) = z_i(t_2)$).

For this case (27) becomes

$$\sin p/p = \acute{A}_i(t_k)\cos(p - \psi_i(t_k)), \qquad k = 1,2 \tag{49}$$

where

$$\acute{A}_i(t_k) = [\|\Delta P_i\|\cos(E_i(t_k))]/(2t_d|\dot{r}_i(t_k)|) \tag{50}$$

and

$$\cos(E_i(t)) = \sqrt{\frac{x_i^2(t) + y_i^2(t)}{x_i^2(t) + y_i^2(t) + z_i^2(t)}}. \tag{51}$$

With $\acute{A}_i(t_k)$ replacing $A_i(t_k)$, the existence and uniqueness analysis is identical to that given earlier.

E. An Example

Assuming noiseless measurements, uniqueness guarantees that the true motion parameters can be found by solving the measurements equations of any feature pair. The motion parameter p and hence $\omega = p/t_d$ are obtained from

$$\sin p/p = A_i(t_k)\cos(p - \psi_i(t_k)), \qquad k = 1,2 \tag{52}$$

using the method of chords given in Appendix A. In general one obtains two values of p for each t. The value of p that satisfies (52) for both $k = 1,2$ is the unique solution.

Once the estimate $\hat{p}$ is obtained, S is estimated by

$$\hat{S} = [P_i(t_1) + P_i(t_2)]/2 + (\cot(\hat{p})/2)B\Delta P_i. \quad (53)$$

For the ith feature, let $P_i(t_1) = [8\ 0]^T$, $P_i(t_2) = [8\ 8]^T$, $\dot{r}_i(t_1) = \pi$, and $\dot{r}_i(t_2) = 0$. Assume $t_d = 1$. The two roots of (52, $k = 1$) are $p = \pi$ and $p = \pi/4$. Similarly, the two roots of (52, $k = 2$) are $p = -3\pi/4$ and $p = \pi/4$. We then set $\hat{p} = \pi/4$ because it satisfies both equations. The center of rotation is located at $\hat{S} = [4\ 4]^T$.

V. SENSITIVITY OF MOTION PARAMETERS TO ERRORS IN MEASUREMENTS

Now consider that the measurements contain noise and the roots of the measurement equations are in error. The measurement equations are barely overdetermined and one would not expect the roots to be highly robust to noise. The use of such roots in an efficient estimator is discussed in [24]. As the density of the measurement errors, estimation bias, and estimation variance are not available, a complete noise analysis is not possible. However, we can calculate the derivative of the motion parameters with respect to the measurements and address the cases for which it is not bounded. Though not totally rigorous, the measurement gradient is composed of reciprocals of the derivatives given here. The measurement gradient is used for calculating the error gradient and Hessian for nonlinear minimization.

Measurement noise can change the parameters of (27) such that roots do not exist particularly if $A_i(t_k)$ is near A_{crit}. We show that the solution $\hat{p}$ can be defined such that the error in the estimate is bounded and goes to zero as the measurement errors go to zero. This is required for nonlinear minimization.

To simplify the derivation, we use the following alternative definitions

$$\overline{A}_i(t_k) = \frac{\|\Delta P_i\|}{2t_d\dot{r}_i(t_k)} \quad (54)$$

$$\overline{\psi}_i(t_k) = \text{sgn}(t_k - t_a)\theta_i(t_k). \quad (55)$$

The equation

$$\frac{\sin p}{p} = \overline{A}_i(t_k)\cos(p - \overline{\psi}_i(t_k)) \quad (56)$$

still holds.

Using the definition of a total derivative for the parameter p,

$$dp = \frac{\partial p}{\partial \Delta P_i}^T d\Delta P_i + \frac{\partial p}{\partial P_i(t_k)}^T dP_i(t_k) + \frac{\partial p}{\partial \dot{r}_i(t_k)} d\dot{r}_i(t_k) \quad (57)$$

it follows that

$$|dp| \le \left\| \frac{\partial p}{\partial \Delta P_i} \right\| \|d\Delta P_i\| + \left\| \frac{\partial p}{\partial P_i(t_k)} \right\| \|dP_i(t_k)\| + \left| \frac{\partial p}{\partial \dot{r}_i(t_k)} \right| |d\dot{r}_i(t_k)|. \quad (58)$$

Here, T denotes the transpose and vector norms are l^2-norms. From (58) it is sufficient to show that

$$\left\| \frac{\partial p}{\partial P_i(t_k)} \right\|, \left\| \frac{\partial p}{\partial \Delta P_i} \right\|, \left| \frac{\partial p}{\partial \dot{r}_i(t_k)} \right| < \infty. \quad (59)$$

Differentiating (56) with respect to the unspecified motion parameter η and also substituting from (56) to remove dependence on $\overline{A}_i(t_k)$ yields

$$\left[\frac{p\cos p - \sin p}{p^2}\cos(p - \overline{\psi}_i(t_k)) + \frac{\sin p}{p}\sin(p - \overline{\psi}_i(t_k)) \right] \frac{dp}{d\eta} = \cos^2(p - \overline{\psi}_i(t_k)) \frac{d\overline{A}_i(t_k)}{d\eta} + \frac{\sin p}{p}\sin(p - \overline{\psi}_i(t_k)) \frac{d\overline{\psi}_i(t_k)}{d\eta}. \quad (60)$$

For $\eta = \Delta P_i$, the partials are

$$\frac{\partial \overline{A}_i(t_k)}{\partial \Delta P_i} = \frac{\sin p \Delta \mathbf{P}_i}{p\cos(p - \overline{\psi}_i(t_k))\|\Delta P_i\|^2} \quad (61)$$

$$\frac{\partial \overline{\psi}_i(t_k)}{\partial \Delta P_i} = \frac{\text{sgn}(t_k - t_a)BR_{\theta_i(t_k)}(1)P_i(t_k)}{\|P_i(t_k)\|\,\|\Delta P_i\|}. \quad (62)$$

The right-hand side of (60) becomes

$$\frac{\sin p}{p\|\Delta P_i\|^2} R_{(p - \overline{\psi}_i(t_k))\text{sgn}(t_a - t_k)}(1)\Delta P_i. \quad (63)$$

We have used the identity

$$P_i(t_k) = \frac{\|P_i(t_k)\|}{\|\Delta P_i\|} R_{\theta_i(t_k)}(1)\Delta P_i. \quad (64)$$

Note that there is a pole at $\|\Delta P_i\| = 0$. If $\|\Delta P_i\| = 0$ we conclude that the motion class $\mathcal{D}_i \in C_2 \cup C_3 \cup C_4$.

For $\eta = \dot{r}_i(t_k)$, it would appear that there are poles at $\dot{r}_i(t_k) = 0$. However, upon more careful examination, poles cancel and the only pole left is the aforementioned pole at $\|\Delta P_i\| = 0$.

For $\eta = P_i(t_k)$, the partials are

$$\frac{\partial \overline{A}_i(t_k)}{\partial P_i(t_k)} = [0\quad 0]^T \quad (65)$$

$$\frac{\partial \overline{\psi}_i(t_k)}{\partial P_i(t_k)} = \frac{\text{sgn}(t_k - t_a)BP_i(t_k)}{\|P_i(t_k)\|^2}. \quad (66)$$

The right-hand side of (60) becomes

$$\frac{\sin p}{p}\sin(p - \overline{\psi}_i(t_k)) \frac{\text{sgn}(t_k - t_a)BP_i(t_k)}{\|P_i(t_k)\|^2}. \quad (67)$$

Thus, there is a pole at $\|P_i(t_k)\| = 0$. The case $\|P_i(t_k)\| = 0$ is easily detected and not expected to occur in practice.

The derivative fails to exist if the coefficient of $dp/d\eta$ in (60) is zero, and the right-hand side is non-zero [25]. This happens when p is the solution of

$$\tan\bar{\psi}_i(t_k) = \frac{p - \sin p \cos p}{\sin^2 p}. \tag{68}$$

Noting that $\tan\bar{\psi}_i(t_k) = \tan\psi_i(t_k)$, this equation is immediately recognized as the definition of the existence boundary. For continuity across the existence boundary we redefine $\hat{p}$ as

$$\hat{p} = \begin{cases} \text{Either solution of } \sin p/p = \bar{A}_i(t_k)\cos(p - \bar{\psi}_i(t_k)) \\ \qquad\qquad \text{if a root exists.} \\ p_{\text{crit}} \qquad\qquad \text{else} \end{cases} \tag{69}$$

Though $dp/d\eta$ does not exist at the boundary, the change in p due to a small error in any measurement is bounded and decreases to zero as the measurement error approaches zero which is illustrated as follows.

Let $\hat{p}^{(0)}$ be the true value of p and let $\hat{p}^{(n)}$ be the calculated parameter from noisy measurements. Then, for any increase in $\dot{r}_i(t_k)$, even if the change causes the roots of the measurement equations to not exist,

$$|\hat{p}^{(n)} - \hat{p}^{(0)}| \le |p_{\text{crit}} - \hat{p}^{(0)}|. \tag{70}$$

Furthermore, $|p_{\text{crit}} - \hat{p}^{(0)}| \to 0$ as the true measurements approach the existence boundary.

But if $\eta = \Delta P_i$ or $P_i(t_k)$, then p_{crit} is affected by the measurements. In this case, let $p_{\text{crit}}^{(0)}$ be the value of p_{crit} without noise and $p_{\text{crit}}^{(n)}$ be the value with noise. Then

$$|\hat{p}^{(n)} - \hat{p}^{(0)}| \le |p_{\text{crit}}^{(0)} - \hat{p}^{(0)}| + |p_{\text{crit}}^{(n)} - p_{\text{crit}}^{(0)}|. \tag{71}$$

The second term may be approximated by

$$p_{\text{crit}}^{(n)} - p_{\text{crit}}^{(0)} \approx \frac{\partial p_{\text{crit}}}{\partial \eta}^{\mathrm{T}} d\eta = \frac{dp_{\text{crit}}}{d\bar{\psi}_i(t_k)} \frac{\partial \bar{\psi}_i(t_k)}{\partial \eta}^{\mathrm{T}} d\eta \tag{72}$$

using the chain rule. The partials of $\bar{\psi}_i(t_k)$ are given in (62) and (66). From (33)

$$\frac{\partial p_{\text{crit}}}{\partial \bar{\psi}_i(t_k)} = \frac{p_{\text{crit}}^2 + \sin^2(p_{\text{crit}}) - 2p_{\text{crit}}\sin(p_{\text{crit}})\cos(p_{\text{crit}})}{2\sin(p_{\text{crit}})(\sin(p_{\text{crit}}) - p_{\text{crit}}\cos(p_{\text{crit}}))}. \tag{73}$$

Both denominator factors have $p_{\text{crit}} = 0$ as their only root on the interval $(-\pi, \pi)$ and

$$\lim_{p \to 0} \frac{\partial p_{\text{crit}}}{\partial \bar{\psi}_i(t_k)} = 3/2. \tag{74}$$

Therefore $|p_{\text{crit}}^{(n)} - p_{\text{crit}}^{(0)}|$ is bounded on that interval.

As $\psi_i(t_k) \to \pm\pi/2$, $p_{\text{crit}} \to \pm\pi$. Furthermore, the derivative in equation (73) tends to infinity at these points. If without noise $|\psi_i(t_k)| > \pi/2$, but due to noise $|\psi_i(t_k)| < \pi/2$, we can redefine $p_{\text{crit}}^{(0)} = \pm\pi$ which is its value at the boundary and equation (71) applies.

Unlike $\hat{p}$ for which the effect of a small change in a measurement is bounded for all interesting cases, an infinitesimally small change in $\hat{p}$ can cause a large change in $\hat{S}$ near $\hat{p} = 0$ or $\pm\pi$. Fortunately, $\hat{p}$ is calculated before $\hat{S}$ so this case is detectable. A trivial remedy is to use the straight-line motion model if $-p_m \le \hat{p} \le p_m$ for some constant p_m. To preclude $\hat{p} = \pm\pi$ (and $\|\Delta P_i\| \approx 0$) one places a lower limit on the data sampling rate. Assuming these constraints have been met, we disregard these cases.

Substituting $P_{a,i} = (P_i(t_2) + P_i(t_1))/2$ in (53) we have

$$\frac{\partial S}{\partial P_{a,i}} = I \tag{75}$$

$$\frac{\partial S}{\partial \Delta P_i} = (\cot(\hat{p})/2)B \tag{76}$$

$$\frac{\partial S}{\partial \hat{p}} = \frac{-1}{2\sin^2(\hat{p})} B\Delta P_i \tag{77}$$

where I is the 2×2 identity matrix. Clearly, no additional poles exist.

VI. CONCLUSIONS

We have shown that unique motion parameters can be obtained from a single feature match for position plus range-rate measurements with the exception of a few specific geometries. Geometric constraints for uniqueness and existence of motion parameters have been given. The motion model uses common motion parameters, parameters that describe the motion of all features associated with a rigid object. Because each feature match (two frames) uniquely determines the motion parameters, motion can be estimated for each feature pair. The result is a significant increase in occlusion tolerance. Finally, the sensitivities of the motion parameters to small changes in measurements are given. All sensitivities are bounded and the errors in motion parameters tend to zero as the measurement errors approach zero.

Several issues must be addressed. Since a single feature association uniquely determines the motion parameters, features may be associated using the common motion paradigm. But, the association of features without a motion estimate has yet to be demonstrated or analyzed. Furthermore, sequential multiple-feature motion estimation with tolerance to errors in feature association needs to be demonstrated. Also, the circular motion model is not adequate for many applications. The model can be extended by allowing the center of rotation to move with constant velocity or allowing the plane of rotation

to be unknown. If the measurements include 3-D position plus Doppler, the motion parameters may be uniquely determined for both extensions. Finally, the theoretical sensitivity analysis needs to be completed and compared with numerical results.

APPENDIX A. FINDING ROOTS OF EQUATION (27)

Section IV shows that (27) has at most two roots on the interval $(-\pi,\pi]$. These roots are also roots of

$$F(p) = A_i(t_k)\cos(p - \psi_i(t_k)) - \sin p/p. \quad (78)$$

We can redefine $F(p)$ as a circular function that wraps around from $-\pi$ to π by constraining its argument to the interval $(-\pi,\pi]$. Since $F(-\pi) = F(\pi)$ the redefined function is continuous.

The method of chords is used to find the roots of $F(\cdot)$ if they exist. This method requires a starting and ending point such that the function, $F(\cdot)$, changes sign on the interval between these points.

First, assume $0 \le |\psi_i(t_k)| < \pi/2$. If roots exist,

$$F(p_{\text{crit}}) = A_i(t_k)\cos(p_{\text{crit}} - \psi_i(t_k)) - \sin p_{\text{crit}}/p_{\text{crit}} \ge 0 \quad (79)$$

equality indicating that both roots are equal to p_{crit}. Note that

$$F(p_{\text{crit}} \pm \pi) < 0. \quad (80)$$

Therefore, we use p_{crit} and $p_{\text{crit}} + \pi$ as the starting and ending points, respectively, in the search for one root and p_{crit} and $p_{\text{crit}} - \pi$ for the other.

Next assume $\pi/2 \le |\psi_i(t_k)| < \pi$. Since two roots are known to exist, no existence test is necessary and p_{crit} is not defined. Here $F(\pi) = F(-\pi) \ge 0$ and $F(0) < 0$. Therefore, we use π and 0 as the starting and ending points, respectively, in the search for one root and $-\pi$ and 0 for the other root.

REFERENCES

[1] Altes, R. A. (1979)
Target position estimation in radar and sonar, and generalized ambiguity analysis for maximum likelihood parameter estimation.
Proceedings of IEEE, 67, 6 (June 1979), 920–930.

[2] Lin, Z. C., Huang, T. S., Blostein, S. D., Lee, H., and Margerum, E. A. (1986)
Motion estimation from 3-D point sets with and without correspondences.
In *Proceedings of IEEE Conference on Computer Vision and Pattern Recognition*, Miami Beach, FL, 1986, 194–198.

[3] Lee, H., and Huang, T. S. (1987)
Three-dimensional motion estimation by synthetic aperture underwater acoustic systems.
In *Proceedings of International Conference on Acoustics, Speech and Signal Processing*, Dallas, TX, Apr. 1987, 1099–1102.

[4] Tsai, R. Y., and Huang, T. S. (1981)
Estimating three-dimensional motion parameters of a rigid planar patch, I.
IEEE Transactions on Acoustics, Speech, and Signal Processing, **ASSP-29** (Dec. 1981), 1147–1152.

[5] ——— (1982)
Estimating three-dimensional motion parameters of a rigid planar patch, II: Singular value decomposition.
IEEE Transactions on Acoustics, Speech, and Signal Processing, **ASSP-30** (Aug. 1982), 525–534.

[6] ——— (1984)
Estimating three-dimensional motion parameters of a rigid planar patch, III: Finite point correspondences and three-view problem.
IEEE Transactions on Acoustics, Speech, and Signal Processing, **ASSP-32** (Apr. 1984), 213–219.

[7] ——— (1984)
Uniqueness and estimation of three-dimensional motion parameters of rigid objects with curved surfaces.
IEEE Transactions on Pattern Analysis and Machine Intelligence, 6 (Jan. 1984), 13–27.

[8] Gennery, D. B. (1982)
Tracking known three-dimensional objects.
In *Proceedings of the National Conference on Artificial Intelligence*, Aug. 1982, 13–17.

[9] Jaenicke, R. A. (1989)
Structure from limited motion of complex rigid objects.
In *Proceedings of the Workshop on Visual Motion*, Mar. 1989, 256–263.

[10] Broida, T. J., and Chellappa, R. (1986)
Estimation of object motion parameters from noisy images.
IEEE Transactions on Pattern Analysis and Machine Intelligence, **PAMI-8** (Jan. 1986), 90–99.

[11] ——— (1986)
Kinematics and structure of a rigid object from a sequence of noisy images.
In *Proceedings of IEEE Workshop on Motion: Representation and Analysis*, May 1986, 95–100.

[12] ——— (1986)
Kinematics of a rigid object from a sequence of noisy images: A batch approach.
In *Proceedings of IEEE Conference on Computer Vision and Pattern Recognition*, Miami Beach, Fl, June 1986, 176–182.

[13] Broida, T. J., Chandrashekhar, S., and Chellappa, R. (1990)
Recursive estimation of 3-D motion from a monocular image sequence.
IEEE Transactions on Aerospace Electronic Systems, 26 (July 1990), 639–656.

[14] Broida, T. J., and Chellappa, R. (1991)
Estimating the kinematics and structure of a rigid object from a sequence of monocular images.
IEEE Transactions on Pattern Analysis and Machine Intelligence, 13, 6 (June 1991), 497–513.

[15] Young, G. S., and Chellappa, R. (1990)
3-D motion estimation using a sequence of noisy stereo images: Models, estimation, and uniqueness results.
IEEE Transactions on Pattern Analysis and Machine Intelligence, 12, 8 (Aug. 1990), 735–759.

[16] Ricks, R. L., and Chatterjee, S. (1988)
A uniqueness proof for sonar motion estimation.
In *Proceedings of the Conference on Information Sciences and Systems*, 1988, p. 211.

[17] ——— (1988)
Recursive Hough transform tracking for sonar motion estimation.
In *Proceedings of the Asilomar Conference on Signals, Systems, and Computers*, Nov. 1988, 440–444.

[18] Chaudhuri, S. (1990)
Feature point based methods for the estimation of three dimensional motion parameters.
Ph.D. dissertation, University of California, San Diego, 1990.

[19] Aggarwal, J. K., and Nandhakumar, N. (1988)
On the computation of motion from sequences of images-a review.
Proceedings of IEEE, 76 (1988), 917–935.

[20] Roecker, J. A., and McGillem, C. D. (1989)
Target tracking in maneuver-centered coordinates.
IEEE Transactions on Aerospace and Electronic Systems, 25 (Nov. 1989), 836–843.

[21] Ziomek, L. J. (1985)
Underwater Acoustics, A Linear Systems Theory Approach.
New York: Academic Press, 1985.

[22] Meiri, A. Z. (1980)
On monocular perception of 3-D moving objects.
IEEE Transactions on Pattern Analysis and Machine Intelligence, PAMI-2 (Nov. 1980), 582–583.

[23] Shensa, M. J. (1981)
On the uniqueness of Doppler tracking.
Journal of the Acoustical Society of America, 70 (Oct. 1981), 1062–1064.

[24] Rousseeuw, P. J., and Leroy, A. M. (1987)
Robust Regression and Outlier Detection.
New York: Wiley and Sons, 1987.

[25] Voxman, W. L., and Goetschel, R. H., Jr. (1981)
Advanced Calculus—An Introduction to Modern Analysis.
New York: Marcel Dekker, 1981.

[26] Ljung, L. (1987)
System Identification: Theory for the User.
Englewood Cliffs, NJ: Prentice-Hall, 1987.

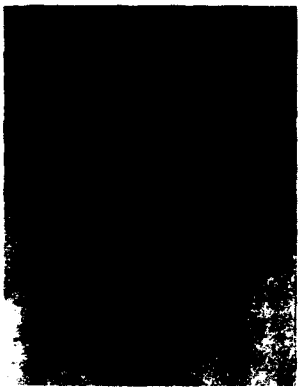

Rockie L. Ricks was born in Sugar City, ID in 1954. He graduated with a B.S. in electrical engineering from Brigham Young University, Summa Cum Laude in 1980 and received an M.E. degree in electrical engineering there in 1981. He is currently working on a Ph.D. at the University of California, San Diego.

Since 1981 he has been employed at Naval Command, Control, and Ocean Surveillance Center, Research, Development, Test, and Evaluation Division, in San Diego, CA. During that time, he has worked on sonar image analysis, tracking, data association, the Hough transform, and waveform design.

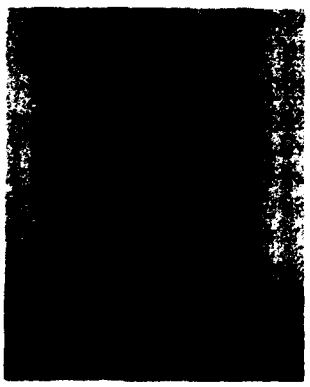

Shankar Chatterjee obtained the B.Tech. (Hons.) degree in electronics and electrical communication engineering from Indian Institute of Technology, Kharagpur, the M.S.E.E. from Louisiana State University, Baton Rough, and the Ph.D. in electrical engineering from University of Southern California, Los Angeles.

He is currently an Assistant Professor in the Electrical and Computer Engineering Department at University of California, San Diego and is in charge of the Computer Laboratory for Analyzing Spatial Signals. His research interests include digital image processing, quantitative vision, estimation theory and stochastic optimization methods.

Dr. Chatterjee was the local Chairman of the IEEE Conference on Computer Vision and Pattern Recognition in 1990.